Realizing Unified Microgrid Voltage Profile and Loss Minimization: A Cooperative Distributed Optimization and Control Approach

Ali Maknouninejad, *Member, IEEE*, and Zhihua Qu, *Fellow, IEEE*

***Abstract*—Cooperative distributed optimization is proposed in this paper to optimally dispatch the reactive power of the distributed generators (DGs). The overall objective is to minimize the cost function that is the sum of all quadratic voltage errors of the DG nodes and other critical nodes in the system. It is assumed that each DG is only aware of its own cost function defined as the quadratic voltage error of its respective node. In the proposed method, every DG performs optimization with respect to its own objective function while considering the information received locally from the neighboring nodes in the microgrid, and the critical nodes without DG also contribute to optimization. The proposed distributed optimization and control scheme enables the microgrid to have a unified voltage profile, and incorporating the subgradient method facilitates its application even when the microgrid information is unknown. Microgrid active power loss is also investigated, and it is shown that the unified voltage profile naturally leads to the overall active power loss minimization as well. Stability analysis and criteria are provided. Simulation results of a typical microgrid illustrate superior performance of the proposed technique.**

***Index Terms*—Cooperative control, distributed generators (DGs), distributed optimization, loss minimization, microgrid, smart grid.**

I. Introduction

To meet the ever increasing demand of energy, the exploit of renewable energy sources and their coupling to the grid, in the form of distributed generators, is gaining more and more attention worldwide. Inverters, due to their fast response and flexibility, are of especial interest in coupling the distributed generators to the grid. These inverters convert the energy harnessed from the various renewable energy sources, such as wind, sun, etc., into a grid quality AC power that can be fed into the utility grid. Usually, the available active power of DGs is less than their nominal capacity. Therefore, the excessive available power generation of DGs may be utilized to produce reactive power, whenever possible. However, a sophisticated control mechanism should be devised to optimally dispatch the individual units reactive power to benefit the overall system performance. As such, the appropriate control and management of inverters will have a significant effect on the performance of a microgrid.

Currently, existing inverter control strategies include current source inverter (CSI) [1], [2], voltage/frequency droop control [3], [4], generator emulation control (GEC) [5], and cooperative control [6]. CSI mainly has the inverter feed all its available power to the grid, without any reactive power generation. It has been shown that CSI may cause stability problems on high penetrations [7].

The highly intermittent nature of renewables is also a source of major concerns. Renewable energy sources, such as solar or wind, are very intermittent in nature. As such, the intermittency of the active power generation by the DGs would be intense. Such intermittency may result in an array of problems, if the DGs control and the reactive power compensation are not coordinated properly. Potential issues are voltage variation [8], [9], transient stability issues, and even voltage collapse [10], [11]. For instance, Fig. 1(a) shows the end point voltage of a short feeder in a typical microgrid,[1] when the solar farm connected to it is exposed to a radiation intermittency as shown in the Fig. 1(b). Such intermittencies are quite normal due to the varying weather conditions, passing clouds, etc. It is noticed how such sun radiation intermittencies directly cause voltage fluctuation.

Therefore, if the CSI control is followed without reactive power generation in high penetrations, such voltage fluctuations could trigger conventional voltage regulators on and off (such as on load tap changers (OLTC) or capacitor banks), and cause conflict. As such, a proper reactive power generation mechanism should be devised to not only prevent such voltage disturbances and conflicts, but also improve the overall system performance.

Different derivatives of the droop control and GEC [12]–[15] use communication-free control to imitate the behavior of the synchronous generators. These controllers regulate their point of connection voltage and frequency. Even though, droop was initially proposed for the parallel operation of the inverters in

Manuscript received January 25, 2014; accepted February 20, 2014. Date of publication April 25, 2014; date of current version June 18, 2014. This work was supported in part by the U.S. National Science Foundation under Grants ECCS-1308928 and CCF-0956501, in part by the U.S. Department of Energy under Award DE-EE0006340 and in part by the Solar Energy Grid Integration Systems (SEGIS) program (phases I to III). Paper no. TSG-00055-2014.

A. Maknouninejad was with the Department of Electrical Engineering and Computer Science, University of Central Florida, Orlando, FL 32816 USA. He is now with Alencon Systems, Inc., Hatboro, PA 19040 USA (e-mail: alimaknouni@knights.ucf.edu).

Z. Qu is with the Department of Electrical Engineering and Computer Science, University of Central Florida, Orlando, FL 32816 USA (e-mail: qu@eecs.ucf.edu).

Color versions of one or more of the figures in this paper are available online at http://ieeexplore.ieee.org.

Digital Object Identifier 10.1109/TSG.2014.2308541

[1]This simulation is based on the feeder 5 of Fig. 5

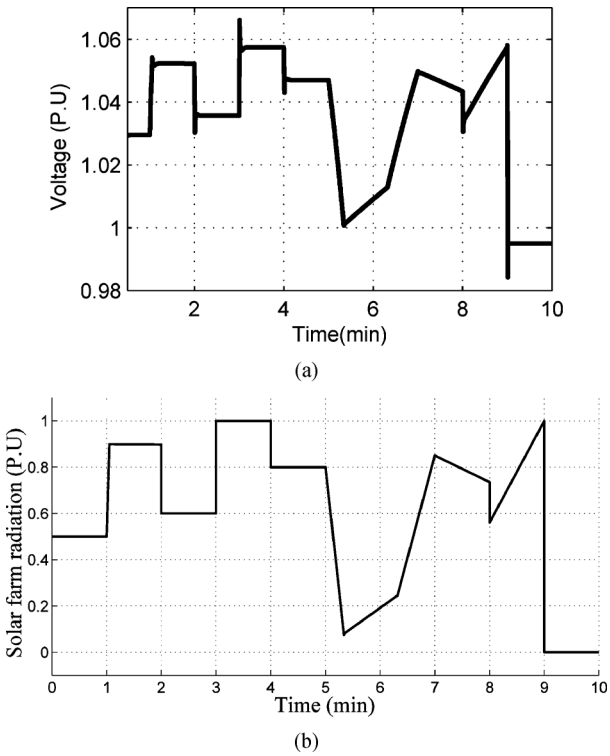

Fig. 1. Voltage disturbance caused by a typical radiation intermittency. (a) Feeder end point voltage. (b) A typical solar radiation intermittency.

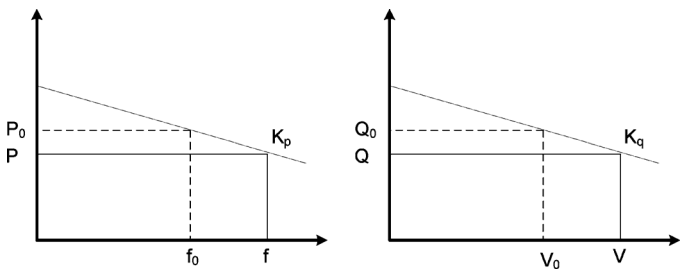

Fig. 2. frequency and voltage droop control characteristics.

the uninterruptable power supplies (UPS) and the islanded microgrid systems [12], [13], [15]; but the application of the droop for the grid connected mode is also proposed [3], [4], [16]–[18].

Droop utilizes the fact that in most power systems, the power angle depends predominantly on P, whereas the voltage difference depends predominantly on Q [12]:

$$f - f_0 = -k_p(P - P_0), \tag{1}$$

$$V_S - V_o = -k_q(Q - Q_0). \tag{2}$$

f_0 and V_0 are the grid rated frequency and voltage, respectively, and P_0 and Q_0 are the (momentary) set points for the active and the reactive power of the inverter. The typical frequency and voltage droop control characteristics are shown graphically in Fig. 2.

In a wide system, with high DG penetration, every DG just regulating its coupling point voltage, could result in an array of problems. For instance, the effect of DG operations on the other parts of the system are neglected. As an illustrative example, in a typical feeder, voltage is the highest at the top, and naturally drops, as going down the line. Droop-based controllers produce a reactive power, proportional to their voltage difference from the unity [19], [20]. As such, the units at the top of the feeder produce less reactive power, while the units at the end of the feeder produce more. That is while, there may be a high reactive power demand on the area as a whole. This non-optimal dispatch of DG's reactive power results in a non-optimal voltage profile across the system and fails to minimize the system losses. Other side effects of the droop-based controllers is the impose of a high reactive power flow to the main grid [21].

Therefore, it is necessary to develop a practical and robust control scheme to properly coordinate DGs together and have them operate cooperatively to secure the demanded power objectives.

The application of the cooperative control on the DG control in the power system was introduced in [6]. It was shown that how cooperative control helps different DGs on the system operate together to realize the designated power objectives. In [6], the reactive power objective was to regulate the voltage of a critical point. This idea was further extended by [21] to clustering DGs into several groups. One group minimizes the reactive power flow to the main grid and others regulate their critical point voltages. It was shown that this multiple critical point regulation could improve the voltage profile across the system.

The application of the cooperative control on maintaining the microgrid voltage and frequency in the islanded mode of operation is discussed in [22]. Furthermore, [23] discussed a decentralized and cooperative architecture for an optimal voltage regulation. The mechanism introduced in [23] is mainly composed of two stages. Initially, through distributed cooperative mechanisms, each unit finds the global cost functions (in terms of the voltage errors and the active power losses). Then, units utilize these information to apply a cooperative optimization. Applying this method could be rather involved and yet there is no stability or convergence proof provided.

This paper particularly applies the cooperative distributed optimization proposed by [24] to the DGs VAR generation control in a typical microgrid. Therefore, the mechanism is easy to implement and the requirement for the units to get an approximation of the global cost functions is relaxed. Each unit only knows about its own cost function and exchanges information locally, with the neighboring units. The detailed stability analysis and proof is also provided. Even though, the focus of this paper is on the grid tied mode, but the same technique may apply to the islanded mode of operation as well.

In the proposed technique, the objective is to minimize the sum of the voltage errors across the microgrid. The global objective is to cooperatively minimize the cost function $\sum_{i=1}^{N} f_i$, where $f_i = (1/2)(1 - V_i)^2$ is the cost function of the ith unit.

The algorithm is as follows: each agent generates and maintains estimates of the optimal decision vector, based on the information concerning his own cost function (in particular, the subgradient information of f_i) and exchanges these estimates directly or indirectly with the other agents in the network. This type of local communication and computation converges to an (approximate) global optimal solution. It is also shown that if there are some critical nodes, without DG installed, but with local measurements and communication modules available, they also can contribute to the optimization.

Having a proper approximation of the line conductances, connecting DG nodes together, is a plus. However, utilization of the subgradient method facilitates the application of this method, even when such detailed information is not available to the DGs. Application of this method will minimize the global cost function, and as such, a unified voltage profile is reached. The power system active power loss is also formulated and is shown that the unified voltage profile, also leads to the overall system active power loss minimization.

The existing voltage regulation devices roughly regulate the node voltages to be within the ANSI standard limits, $\pm 5\%$. However, it is advantageous to take use of the DGs in improving the voltage quality. In this paper, it is shown how the DGs reactive power generation capacity can be utilized to further regulate voltages and achieve a more unified voltage profile. It is also shown that a unified voltage profile yields loss minimization. Furthermore, a unified voltage profile around the unity provides a larger safe zone for the voltage swing, which may be caused by any potential system disturbance.

The rest of the paper is organized as follows. The problem formulation is presented in the Section II. The proposed cooperative distributed optimization method is proposed in the Section III. Section IV formulates the real power loss of the system and shows how a unified voltage profile results in the loss minimization. The related convergence and stability analysis is also provided in Appendix A. The provided simulation results demonstrate the effectiveness of the proposed optimization method.

II. Problem Formulation

Usually the active power generated by the inverters is less than their power ratings. As such, the remaining capacity of the inverters may be utilized to generate reactive power. The proper reactive power control of DGs is a challenge and results in the system voltage profile improvement and the loss minimization.

The application of the cooperative control to manage the reactive power generation of DGs in a microgrid to satisfy multiple objectives was explored in [21]. It was suggested by [21] to cluster the DGs into several groups to regulate multiple critical points voltages and minimize the aggregated reactive power flow to the main grid. To facilitate the equal contribution of DGs into the reactive power generation, a reactive power fair utilization ratio, α_q, is defined as follows:

$$\begin{aligned} \overline{Q}_i &= \sqrt{S_i^2 - P_i^2} \\ \alpha_{q_i} &= \frac{Q_i}{\overline{Q}_i} \end{aligned} \tag{3}$$

where S_i, P_i, Q_i, and $\overline{Q}_i$ are the power rating, generated active power, generated and the maximum available reactive power of the ith unit respectively. The reactive power fair utilization ratio determines how much percentage of the available reactive power should be generated by each DG.

As suggested by [21] and [6], each group has a virtual leader. The virtual leader may be a DG that has access to the higher level control, or the related power flow and voltage information. As such, the virtual leader can calculate the required utilization ratio to realize the desired power objective. As discussed in [6],

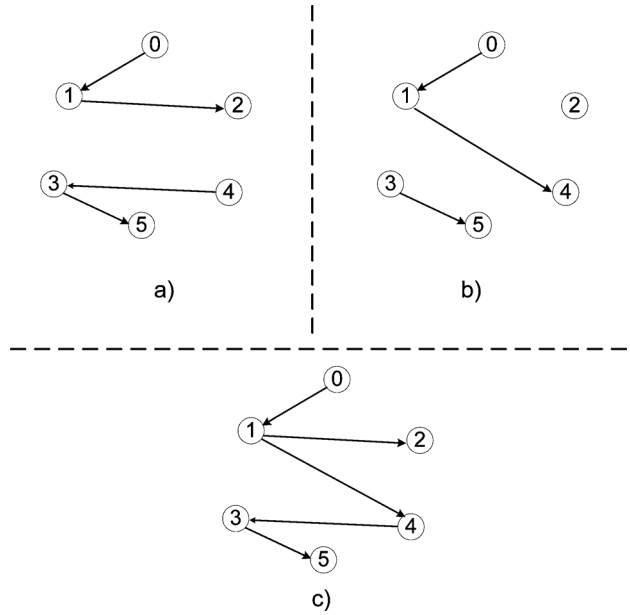

Fig. 3. Cumulative connectivity. (a) Communication graph at t_k. (b) Communication graph at t_{k+1}. (c) Cumulative communication graph from t_k to t_{k+1}.

an integrator controller may be used by the virtual leader to update the α_q^{ref} as follows:

$$\dot{\alpha}_q^{\mathrm{ref}} = k_q(V^{\mathrm{ref}} - V_{cp_i}) \tag{4}$$

where V_{cp_i} and V^{ref} are the ith critical point voltage and the reference voltage respectively. Parameter k_q is a control gain, and typically $V^{\mathrm{ref}} = 1\ \mathrm{PU}$.

DGs should utilize communication links to communicate and converge to the same operating point, α_q^{ref}, provided by the virtual leader [6], [25]. The instantaneous communication topology is defined by the following matrix:

$$S(t) = \begin{bmatrix} s_{00}(t) & s_{01}(t) & s_{02}(t) & \cdots & s_{0N}(t) \\ s_{10}(t) & s_{11}(t) & s_{12}(t) & \cdots & s_{1N}(t) \\ s_{20}(t) & s_{21}(t) & s_{22}(t) & \cdots & s_{2N}(t) \\ \vdots & \vdots & \vdots & \ddots & \vdots \\ s_{N0}(t) & s_{N1}(t) & s_{N2}(t) & \cdots & s_{NN}(t) \end{bmatrix}. \tag{5}$$

In (5), $s_{ii} = 1$ for all i; $s_{ij} = 1$ if the output of the jth DG is known to the ith DG at time t, and $s_{ij} = 0$ if otherwise. In (5), unit (0) is assumed to be the virtual leader. The minimum requirement for the communication network is that it should be connected over the time and it should be either strongly connected (which implies that, by following the directed branches, every node can be reached from any other node) or there be a globally reachable node (in the sense that all other nodes can be reached from the globally reachable node by following the directed branches of the graph [26]). Fig. 3 further illustrates the concept of the cumulative connectivity. Neither Fig. 3(a), nor Fig. 3(b), are connected. However, if these two communication networks happen consecutively, the resulting effect yields a cumulative connected graph over time, as shown by Fig. 3(c)

The closed-loop cooperative control law for the ith DG is as follows [26]:

$$\alpha_{q_i}(k+1) = \sum_{j=1}^{N} d_{ij}\alpha_{q_j}(k) + d_{i0}\alpha_q^{\mathrm{ref}} \tag{6}$$

where

$$d_{ij} = \frac{\omega_{ij} s_{ij}}{\sum_{l=0}^{N} \omega_{il} s_{il}}, \quad i, j = 0, 1, \ldots N. \tag{7}$$

$\omega_{ij} > 0$ are the weights. For a symmetric system, all $\omega_{ij} = 1$.

In this paper, it is proposed to regulate the voltage of all the DGs across the microgrid, rather than just some critical points. This yields a unified voltage profile and as will be shown, the unified voltage profile will also result in the loss minimization as well. As such, there is no need to define distinctive cost functions or cluster DGs differently for the voltage regulation and the loss minimization. Following this scheme, the need of the virtual leader is relaxed and each unit tries to find its best operating point, α_{q_i}, while exchanging information locally with others. The design details of this cooperative law is the problem to be addressed on the next section.

III. Cooperative Control Based on the Distributed Optimization

The design objective is for the DGs to cooperatively control their reactive power injection toward minimizing the following objective:

$$F_v = \sum_{i=1}^{N} f_{v_i}, \qquad f_{v_i} = \frac{1}{2}(1 - V_i)^2. \tag{8}$$

Should the voltages be known globally by all the DG units, optimal control could be designed to minimize objective function (8), by simply calculating the gradient of F_v with respect to α_q. Since global information is not available, the distributed optimization and control has to be used [24].

The control variables are DGs reactive power fair utilization ratios. The information state of the ith DG, α_{q_i} is an estimate of an optimal solution of the problem (8). The variable $\alpha_{q_i}(k)$ is the estimate, maintained by the agent i, at the time t_k. When generating a new estimate, unit i combines its current estimate, α_{q_i}, with the estimates received from some of the other neighboring units. In particular, unit i updates its estimates according to

$$\alpha_{q_i}(k+1) = \sum_{j=1}^{N} d_{ij} \alpha_{q_j}(k) - \beta_i g_i \tag{9}$$

where d_{ij} is defined by (7), $\beta_i > 0$ is a step size gain, used by the agent i, and the parameter g_i is a gradient (or a subgradient) of the ith DG objective function, f_{v_i}, in respect to its state, α_{q_i}.

Traditionally, voltage control is coarsely done by the means of OLTC and/or switches of capacitor banks (CBs). DGs can be used as either an auxiliary source of the reactive power to provide fine control of voltage or a primary source of reactive compensation (given a sufficient level of DG penetration). It is assumed without loss of any generality that both capacitor banks (or OLTC) and DGs are present with a comparable generation capacity (otherwise simple scaling factors could used to make their capacities comparable). Then, the proposed cooperative control methodology can readily be applied except that, if the ith control is for either capacitor banks or an OLTC, its discrete control action requires that control (9) be modified to be the following:

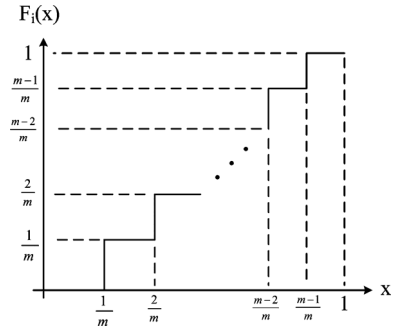

Fig. 4. Stair function employed in the control for of OLTC or capacitor banks.

$$\alpha_{q_i}(k+1) = F_i\left(\sum_{j=1}^{N'} d_{ij} \alpha_{q_j}(k) - \beta g_i\right) \tag{10}$$

where N' is the total number of the reactive power compensation devices, $F_i(\cdot)$ is the stair function shown in Fig. 4, and m is the number of available step changes in the OLTC or capacitor bank. Note that DG controls can act much faster than those of the OLTCs and/or capacitor banks, and hence the stair function $F_i(\cdot)$ in Fig. 4 also reinforces this inherent two-time-scale separation of DG controls and OLTC/CB controls. To avoid any possible chattering in OLTC/CB control actions, a simple hysteresis or a low-pass filter or both can further be incorporated into function $F_i(\cdot)$.

As seen by (9) and (10), the only variable that units need to exchange is their reactive power fair utilization ratio, α_{q_i}. As already discussed on [6], application of such cooperative control does not need much communication. Actually, exchanging information locally, within the neighboring units is sufficient [6], [26]. It is distinctive that the proposed control can tolerate the changes in the distribution network, its local communication network can be intermittent with delays and have time varying topologies, and its communication bandwidth can be of minimum. As it was extensively discussed in [27] and [28], time delays would not jeopardize stability or convergence, albeit the speed of the convergence would be impacted by the amount of delays.

The parameter g_i in (9) is calculated as follows for DGs or nodes in different situations:

- For a node with DG and known B_{ii}:

$$g_i = -\overline{Q}_i(1 - V_i)\frac{V_i}{Q_i - V_i^2 B_{ii}}. \tag{11}$$

- For a node with DG, but unknown B_{ii}:

$$g_i \to g_i' = \begin{cases} -\overline{Q}_i(1 - V_i)\frac{V_i}{Q_i - V_i^2 \overline{B_{ii}}}, & V_i \le 1; \\ -\overline{Q}_i(1 - V_i)\frac{V_i}{Q_i - V_i^2 \underline{B_{ii}}}, , & V_i > 1. \end{cases}. \tag{12}$$

- For a node without DG:

$$g_i = -x_i(1 - V_i)\frac{V_i}{Q_i - V_i^2 B_{ii}} \tag{13}$$

where $B_{ii} \in [\underline{B}_{ii}, \overline{B}_{ii}]$ is the sum of the imaginary parts of the line conductances, connecting node i to the neighboring nodes, g_i' is a subgradient of g_i and x_i is the average of the all units available reactive power on the system.

The derivations of the individual gradients are explicitly carried out in Sections III-A and III-B. The discussion on the selection of the gradient gains, β, is provided in Section III-C. The convergence and the stability analysis of (9) are also provided in Appendix A.

A. Gradient Calculation for DG Nodes

Considering (3) and (8) yields

$$\begin{aligned} g_i &= \frac{\partial f_{v_i}}{\partial \alpha_{q_i}} \\ &= \frac{\partial f_{v_i}}{\partial V_i}\frac{\partial V_i}{\partial Q_i}\frac{\partial Q_i}{\partial \alpha_{q_i}} \\ &= -\overline{Q_i}(1-V_i)\frac{\partial V_i}{\partial Q_i}. \end{aligned} \tag{14}$$

The system power flow equations are expressed as follows:

$$\begin{cases} P_{G_i} - P_{D_i} = \sum_{j=1}^{N} V_i V_j [G_{ij}\cos\delta_{ij} + B_{ij}\sin\delta_{ij}] \\ Q_{Gi} - Q_{Di} = \sum_{j=1}^{N} V_i V_j [G_{ij}\sin\delta_{ij} - B_{ij}\cos\delta_{ij}] \end{cases} \tag{15}$$

where δ_{ij} is the phase difference between nodes i and j. Quantities B_{ij} and G_{ij} are the real and imaginary parts of the system Y bus matrix. Symbols $P_{G_i}, P_{D_i}, Q_{G_i}$ and Q_{D_i} are the ith node active power generation, active power load, reactive power generation and reactive power load, respectively.

The reactive power flow in (15) may be rewritten as follows:

$$\begin{aligned} Q_i = Q_{Gi} - Q_{Di} &= \sum_j V_i V_j [G_{ij}\sin\delta_{ij} - B_{ij}\cos\delta_{ij}] \\ &= -V_i^2 B_{ii} + V_i \sum_{j\neq i} V_j [G_{ij}\sin\delta_{ij} - B_{ij}\cos\delta_{ij}]. \end{aligned} \tag{16}$$

From (16), the required gradients can be derived as follows:

$$\begin{aligned} \frac{\partial Q_i}{\partial V_i} &= -2V_i B_{ii} + \sum_{j\neq i} V_j [G_{ij}\sin\delta_{ij} - B_{ij}\cos\delta_{ij}] \\ &= -V_i B_{ii} + \frac{Q_i}{V_i}. \end{aligned} \tag{17}$$

Plugging (17) into (14) yields the gradient term of (11)

The (11) implies that the only system information needed is B_{ii}, that is the sum of the imaginary parts of the line conductances, connecting node i to the neighboring nodes. However, if this information is not available to the DGs, a subgradient of (11), g_i', may be used instead [24]. In a particular power system, the lengths of the lines and their impedances have to be in a certain numerical range. Based on such information, upper and lower bounds of B_{ii} can be calculated, $B_{ii} \in [\underline{B}_{ii}, \overline{B}_{ii}]$. Therefore, by definition, the subgradient of (11) is given by (12).

B. Gradient Calculation for Non-DG Nodes

If there is no DG installed on a node, then the $\overline{Q}_i$ of that node is zero. This makes the gradient/subgradient defined by (11) or (12) zero, and hence, such modules will not contribute into the optimization. For these nodes, the definition of the virtual leader as discussed in Section II is applied. Typically, a virtual leaders tries to regulate the voltage of its respective node by utilizing all other units reactive power capacity.

For the cooperative distributed optimization discussed here, the same concept of a virtual leader may be applied to the nodes without a DG installed. That means they should utilize the other units reactive power generation to regulate their respective node. As such, the $\overline{Q}_i$ in (11) will be replaced by the average of all the units available reactive power capacity.

As the optimization is being performed, units may utilize the same communication links to find the average of all units available reactive power capacity as well. Every unit tries to keep the track of the average by a state, x_i. The initial value of x_i is the units available reactive power. Units update their states, according to the following cooperative law:

$$x_i(k+1) = \sum_{j=1}^{N} d_{ij}' x_j. \tag{18}$$

$d_{ij}' = 0$, provided that $s_{ij} = 0$. Similar to $D = [d_{ij}]$ matrix, defined by (7), $D' = [d_{ij}']$. However, D' should be designed to be double stochastic [26]. That is

$$\begin{cases} D'\mathbf{1} = \mathbf{1}, \\ \mathbf{1}^T D' = \mathbf{1}^T \end{cases}$$

where $\mathbf{1}$ is a $N \times 1$ vector, with all elements equal to one. Following the law in (18), results in all the states, x_i, converge to the desired value:

$$x_i \to \frac{1}{N}\sum_{j=1}^{N} \overline{Q_i}.$$

Hence, the gradient term of (11) for such units is formulated as (13).

C. Choosing the Gradient Gains, β

The β gains in (9) should be chosen in such a way to give the best performance. Heuristically, small gains will slow down the pace of the distributed optimization; and on the other hand, large gains tend to introduce overshoots that induce oscillations, and even may cause system instability on extremes.

Theorem 2 of Appendix A shows that for a particular power system, there exists a range of the β, which secures the system stability. This theorem may be used to numerically calculate the desired β gains, or equivalently, a best choice of β may be found out by running the simulations.

IV. Active Power Loss Analysis

Theorem 1: A unified microgrid voltage profile also results in the system active power losses minimization.

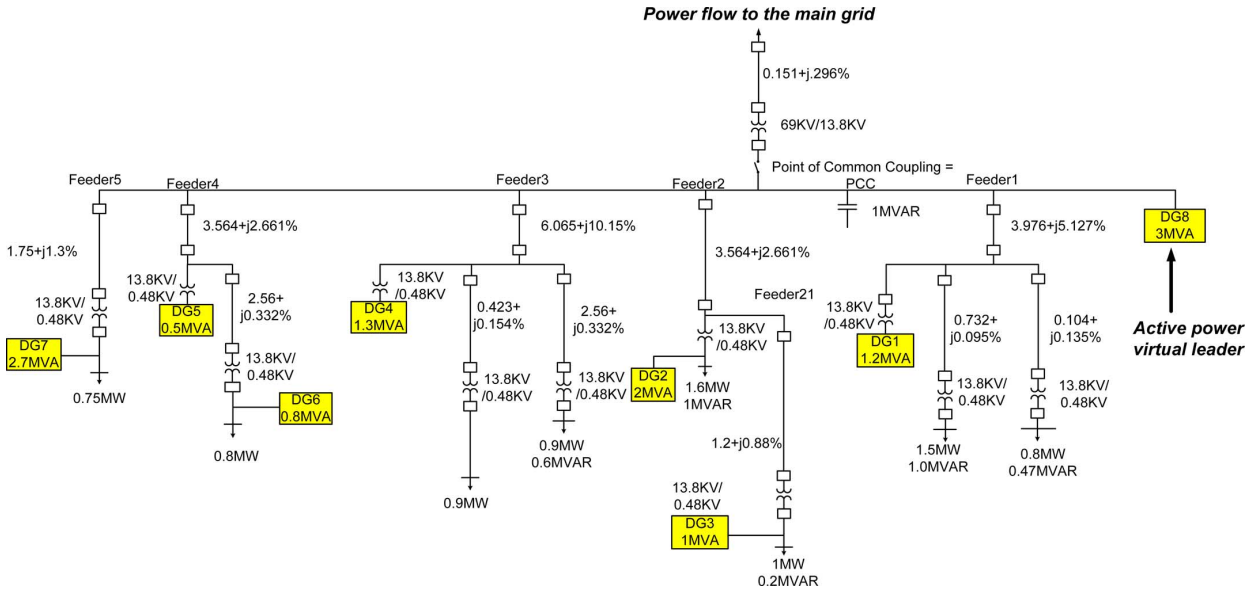

Fig. 5. System diagram of the case of study microgrid.

Proof: The current flowing between two nodes, i and j, in a power system, is expressed as

$$I_{ij} = (V_i \angle\theta_i - V_j \angle\theta_j)(G_{ij} + jB_{ij}).$$

The complex power over the line is

$$\begin{aligned} s_{Lost_{ij}} &= (V_i \angle\theta_i - V_j \angle\theta_j) I_{ij}^*, \\ &= (V_i \angle\theta_i - V_j \angle\theta_j)(V_i \angle -\theta_i - V_j \angle -\theta_j)(G_{ij} - jB_{ij}), \\ &= (V_i^2 + V_j^2 - 2V_i V_j \cos(\theta_i - \theta_j))(G_{ij} - jB_{ij}). \quad (19) \end{aligned}$$

In the power systems, usually the phase difference between two adjacent nodes is close enough to approximate its cosine to be unity, i.e., $\cos(\theta_i - \theta_j) \simeq 1$. Therefore, active power loss in the ij branch can be evaluated based on (19) as follows:

$$P_{Loss_{ij}} \simeq G_{ij}(V_i - V_j)^2. \quad (20)$$

Therefore, the system total losses is as follows:

$$P_{Loss} = \sum_{i=1}^{N-1} \sum_{j=i+1}^{N} G_{ij}(V_i - V_j)^2. \quad (21)$$

Equation (21) shows that the power losses of the system are proportional to the voltage differences among the adjacent nodes. As such, realizing a unified voltage profile across the microgrid will result in the loss minimizations as well. ■

V. Simulation Results

A modified version of the bus system proposed by the IEEE 399-1997 standard is used to represent the microgrid case of study, as shown in the Fig. 5. The power base is 10 MVA in this figure. Simulations are performed using the Simpower System Toolbox of Simulink. Main grid is 69 KV and the microgrid consists of five 13.8-KV distribution feeders. Eight DGs are distributed across the microgrid with a total of 15.5-MVA generation capacity. DGs 2, 3, and 4 are wind farms and DGs 1, 5, 6, 7, and 8 are solar farms. The DG profiles are shown in Fig. 6. The weather effect and sun radiation intermittencies are

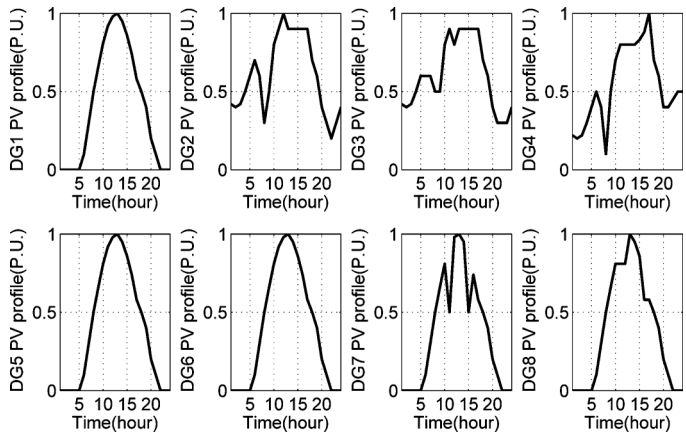

Fig. 6. Profile of DGs.

considered in these profiles. The total load is 8.25 MW + 2.27 MVAR. Loads and DGs operate on a lower voltage of 430 V. A 1 MVAR capacitor bank is connected to the point of common coupling (PCC), and the bank consists of five 200-KVAR capacitors. Simulations are performed for the time period of 9:00 AM up to 6:00 PM.

Three different microgrid inverter control schemes, droop, multiple critical points voltage regulation, and the cooperative distributed optimization, proposed by this paper, are evaluated. The performance of these controllers in realizing the microgrid power objectives are compared.

In droop, every DG just regulates its grid coupling point voltage and frequency. Other two techniques utilize communication links and the cooperative control. To provide a fair comparison between the evaluated techniques, the active power policy is chosen to be identical, to regulate the power flow from the main grid at 2.5 MW. DG8, is the active power virtual leader. For the reactive power control, DGs are controlled as follows. In multiple critical points regulation, DGs are clustered into three groups. The first group, consisting of DGs 7, and 8, minimizes the reactive power flow to the main grid. The

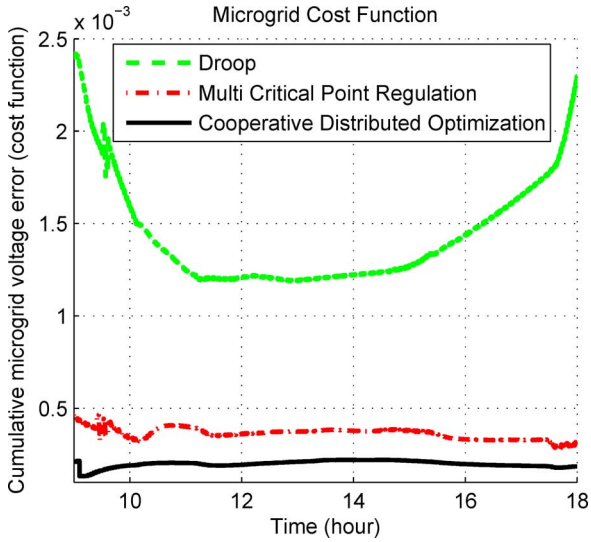

Fig. 7. Global cost function of the microgrid, F_v.

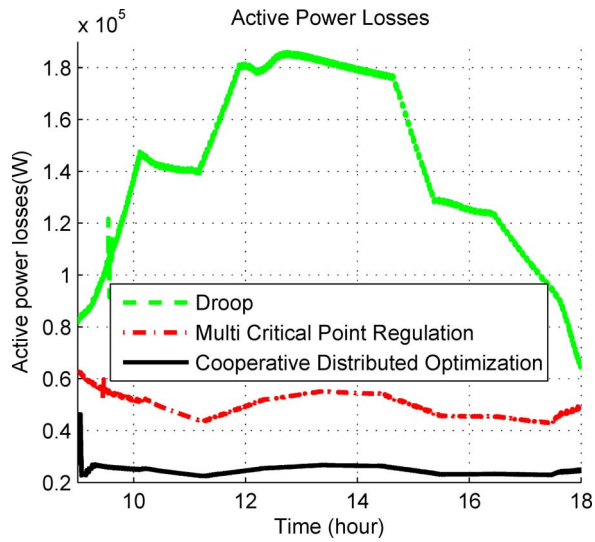

Fig. 9. Microgrid active power loss.

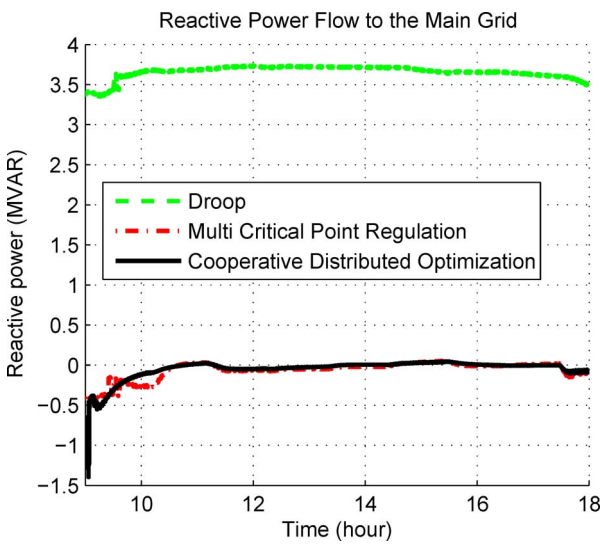

Fig. 8. Main grid reactive power flow to the microgrid.

second group, DGs 1, 2, and 3, regulate the DG3 voltage, as a critical point. The third group, DGs 4, 5, and 6, regulate the other critical point, DG6.

In the cooperative distributed optimization, similar to the multiple critical points regulation, DGs 7 and 8 minimize the aggregated reactive power flow to the main grid. All other DGs participate in the distributed optimization to cooperatively minimize the sum of their nodes voltage error, which is expressed by the cost function (8) with $n = 6$. The gradient gains have been chosen as $\beta_i = 15$ for all the DGs in this simulation.

The capacitor bank is controlled according to the proposed cooperative distributed optimization law (10). For the droop and multiple critical points regulation, a traditional capacitor bank control is adopted; that is, the number of the capacitors switched on is directly proportional to the voltage drop. In other words, all the capacitors are turned on when the sampled voltage is at 0.95 PU, and all are disconnected when the voltage is at unity. The sampling point for the capacitor bank control is DG3 node, which is a critical point.

Simulation results are provided in Figs. 7–10. Fig. 7 shows the system cost function, F_v. It is seen that the droop achieves the highest value of the cost function, while the cooperative distributed optimization has well minimized it, and as such, has realized the most unified voltage profile.

Fig. 8 shows the main grid reactive power flow to the microgrid. It is clear that droop has induced a high reactive power to the main grid, while cooperative control techniques successfully have minimized it, despite the intermittencies.

Fig. 9 shows the system active power losses. The cooperative distributed optimization has realized the minimum losses and the droop has led to the highest loss. This certifies the previous discussion that a more unified voltage profile results in a lower active power loss.

Fig. 10 shows the voltages at two different system nodes, point of common coupling (PCC) and DG6 terminals. This figure illustrates how cooperative distributed optimization has maintained a unified voltage profile, close to unity, across the microgrid. Also it is notable that this technique well regulates and maintains the voltages despite the daily intermittencies. The other point learned from this figure is that droop fails to keep the voltage at different nodes as close. That means a non-unified voltage profile, as already was shown by Fig. 7. Also, the sun radiation intermittencies have caused major voltage fluctuations, when DGs are controlled by the droop.

Fig. 11 illustrates outcomes of the capacitor bank operation. It is seen that both the droop and the multiple point regulation schemes cause the capacitor bank to experience two consecutive on/off switchings during time interval of 9:00–10:00 A.M. and to settle down at a reactive power generation value less than what the microgrid needs. In comparison, the capacitor bank operation is stable under the proposed cooperative distributed optimization, and the capacitor bank is also better utilized since the proposed algorithm implicitly realizes that more reactive power generation is needed and it keeps the same number of capacitors on during the whole period.

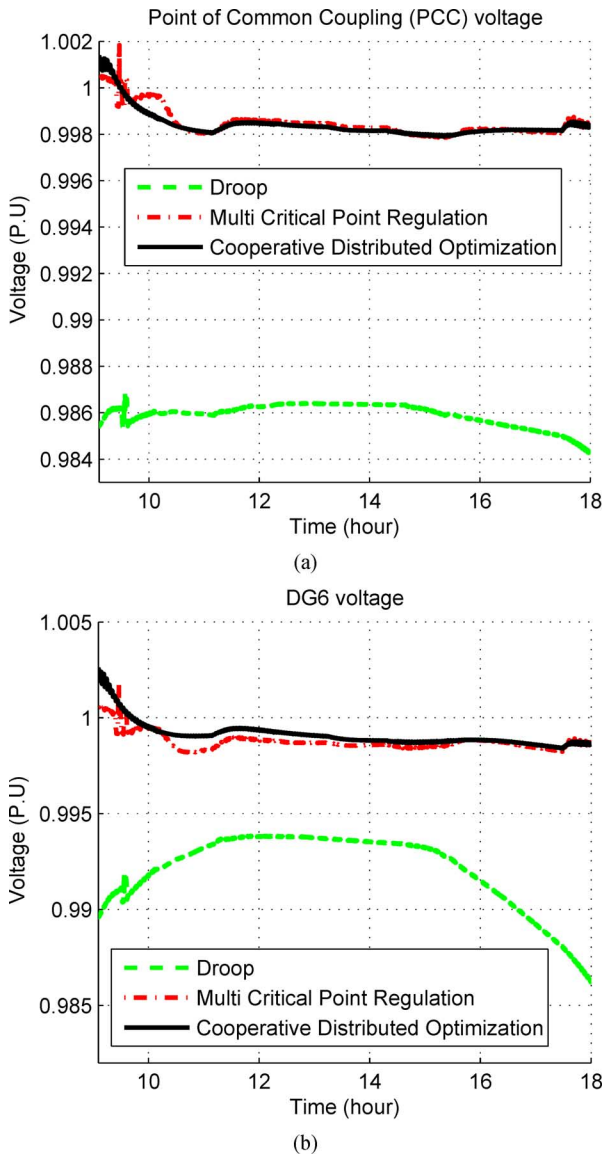

Fig. 10. Voltages of DG6 and point of common coupling. (a) Voltage of point of common coupling. (b) Voltage of DG6.

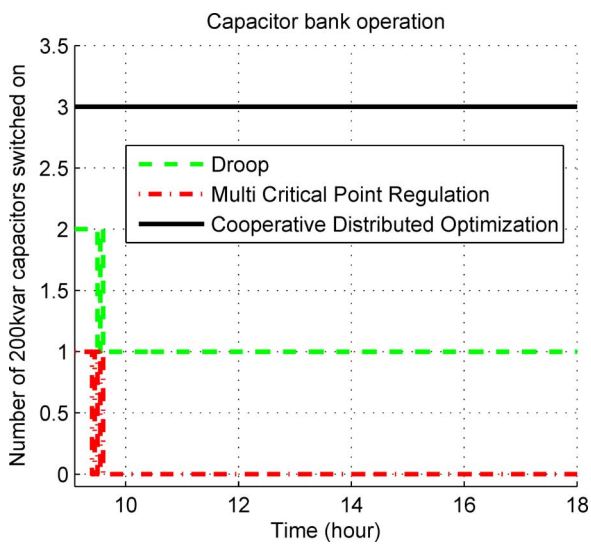

Fig. 11. Number of capacitors of the capacitor bank switched on.

VI. Conclusion

In this paper, the application of the cooperative distributed optimization to optimally dispatch the reactive power generation of DGs in a microgrid is investigated. The main objective is to realize a unified microgrid voltage profile.

In a large-scale microgrid, there may be some critical nodes without a DG installed, but with the required measurements and communication modules available. A method also is provided to facilitate the contribution of such nodes in the optimization process.

The only system information required to implement this technique is an approximation of the line conductances, connecting DG nodes together. However, it is shown that the application of the subgradient technique makes it possible to use this method, even when such detailed information is not available.

The system active power losses are also formulated, and it is shown that how a unified voltage profile results in the loss minimization as well. The stability and the convergence analysis are also provided.

The simulation results applied to a typical microgrid are provided. It is shown that, despite of the daily PV intermittencies, the proposed technique realizes a unified microgrid voltage profile, lower losses, and better operation and control of capacitor banks. These results are superior to those under the state of the art microgrid inverter controls.

Appendix
Analysis

This section investigates the convergence and the stability analysis of the proposed distributed cooperative optimization. The materials provided in this section, including the linearization and other discussions, are not needed to run the proposed control; which was fully provided on the Section III.

To analyze the system, it is required to express the gradient term in (9) in terms of the system states, α_{q_i}. Therefore, let's linearize the gradient term of (11), g_i, around the optimal operating point, V_i^* and $\alpha_{q_i}^*$:

$$g_i(V_i,\alpha_{q_i}) \simeq g_i^* + e_i(V_i - V_i^*) + f_i(\alpha_{q_i} - \alpha_{q_i}^*) \tag{22}$$

where $g_i^* = g_i(V_i^*, \alpha_{q_i}^*)$ and utilizing (11)

$$\begin{aligned} e_i &= \frac{\partial g_i(V_i,\alpha_{q_i})}{\partial V_i}\Big|_{V_i^*\&\alpha_{q_i}^*} \\ &= -\overline{Q}_i \frac{\alpha_{q_i}\overline{Q}_i(1-2V_i) + V_i^2 B_{ii}}{(\alpha_{q_i}\overline{Q}_i - V_i^2 B_{ii})^2}\Big|_{V_i^*\&\alpha_{q_i}^*} \end{aligned} \tag{23}$$

and

$$\begin{aligned} f_i &= \frac{\partial g_i(V_i,\alpha_{q_i})}{\partial \alpha_{q_i}}\Big|_{V_i^*\&\alpha_{q_i}^*} \\ &= \overline{Q}_i{}^2 \frac{V_i(1-V_i)}{(\alpha_{q_i}\overline{Q}_i - V_i^2 B_{ii})^2}\Big|_{V_i^*\&\alpha_{q_i}^*}. \end{aligned} \tag{24}$$

Also, linearizing the system power flow (15) around the optimal operating points, provides

$$\begin{bmatrix} P - P^* \\ \alpha_q - \alpha_q^* \end{bmatrix} = H \begin{bmatrix} V - V^* \\ \delta - \delta^* \end{bmatrix} \tag{25}$$

where $P = [P_1, \ldots, P_N]^T$, $V = [V_1, \ldots, V_N]^T$, $\alpha_q = [\alpha_{q_1}, \ldots, \alpha_{q_N}]^T$, $\delta = [\delta_1, \ldots, \delta_N]^T$, and H is the Jacobian matrix. Then it follows that

$$\begin{bmatrix} V - V^* \\ \delta - \delta^* \end{bmatrix} = \begin{bmatrix} H_{11} & | & H_{12} \\ - & . & - \\ H_{21} & | & H_{22} \end{bmatrix} \begin{bmatrix} P - P^* \\ \alpha_q - \alpha_q^* \end{bmatrix} \quad (26)$$

where

$$\begin{bmatrix} H_{11} & | & H_{12} \\ - & . & - \\ H_{21} & | & H_{22} \end{bmatrix} = H^{-1}.$$

Substituting (22) in (9) yields

$$\begin{aligned} &\alpha_{q_i}(k+1) \\ &= \sum_j d_{ij}\alpha_{qj}(k) - \beta_i g_i, \\ &= \sum_j d_{ij}\alpha_{qj}(k) - \beta_i \left[g_i^* + e_i(V_i - V_i^*) + f_i(\alpha_{q_i} - \alpha_{q_i}^*)\right]. \end{aligned} \quad (27)$$

Equation (27) may be written in the matrix format as follows:

$$\alpha_q(k+1) = D\alpha_q(k) - \beta[g^* + E(V - V^*) + F(\alpha_q - \alpha_q^*)] \quad (28)$$

where $D = [d_{ij}]$ is a row stochastic matrix. Also $g^* = [g_1^*, \ldots, g_N^*]^T$, $E = diag(e_i)$, $F = diag(f_i)$, and the gain $\beta = diag[\beta_1, \ldots, \beta_N]$. The parameter g^* can be calculated by evaluating (28) at the optimal operating point, α_q^* and V^*:

$$\alpha_q^* = D\alpha_q^* - \beta g^* \Rightarrow g^* = -\beta^{-1}(I - D)\alpha_q^* \quad (29)$$

where I is a $N \times N$ unity matrix.

Substituting g^* and $V - V^*$ from (29) and (26) respectively in (28) provides

$$\begin{aligned} &\alpha_q(k+1) = [D - \beta(EH_{12} + F)]\alpha_q(k) \\ &+[(I - D) + \beta(EH_{12} + F)]\alpha^* - \beta EH_{12}(P - P^*). \end{aligned} \quad (30)$$

If P is not constant, then N extra independent active power states are introduced in (30). These states are independent of the states of interest, α_q. Hence, the stability and the dynamic response of the proposed optimization method is absolutely independent of these active power states. As such, for the simplicity and without loss of the generality, the active power flow, P, is assumed to be constant at P^*. Therefore, (30) may be reformatted as follows:

$$\alpha_q(k+1) - \alpha_q^* = [D - \beta(EH_{12} + F)](\alpha_q(k) - \alpha_q^*). \quad (31)$$

The stability and the convergence rate of the system depend on the state matrix, $D - \beta(EH_{12} + F)$, and are based on the following lemmas and theorem:

Lemma 1: If the eigenvalues of the row-stochastic and connected matrix D are denoted as λ_i with $\lambda_1 = 1 > \lambda_2 \geq |\lambda_j|$ for $j = 3, \ldots, N$, then matrix

$$A' = D - c\mathbf{1}\boldsymbol{\gamma}^{\mathbf{T}} \quad (32)$$

with scalar $c \in (0, 2]$ has eigenvalues of $(1 - c)$ and λ_i for $i = 2, \ldots, N$. Quantity γ is the left eigenvector of D, corresponding to the left eigenvalue of 1 (γ is scaled as: $\gamma^T\mathbf{1} = 1$).

Proof: Let ξ_i denotes the eigenvector corresponding to λ_i for $i = 2, \ldots, N$. Therefore,

$$\begin{cases} \gamma^T D\xi_i = \gamma^T(D\xi_i) = \lambda_i\gamma^T\xi_i \\ \gamma^T D\xi_i = (\gamma^T D)\xi_i = \gamma^T\xi_i \end{cases} \Rightarrow \gamma^T\xi_i = 0.$$

It follows that

$$A'\mathbf{1} = D\mathbf{1} - c\mathbf{1}\gamma^T\mathbf{1} = (1 - c)\mathbf{1}$$

and

$$A'\xi_i = D\xi_i - c\mathbf{1}\gamma^T\xi_i = \lambda_i\xi_i,$$

which completes the proof. ■

Lemma 2: $EH_{12} + F$ is a positive matrix.

Proof: Using the approximation of $V_i^* \simeq 1$, (23) may be simplified as follows:

$$e_i \simeq -\overline{Q}_i \frac{-\alpha_{q_i}\overline{Q}_i + B_{ii}}{(\alpha_{q_i}\overline{Q}_i - B_{ii})^2}\Big|_{V_i^* \& \alpha_{q_i}^*}. \quad (33)$$

In (33), $-1 < \alpha_{q_i} < 1$ and $0 < \overline{Q}_i < 1$, as all the calculations are in the per unit. This implies that $-1 < \alpha_{q_i}\overline{Q}_i < 1$. Furthermore, in power systems usually line impedances, especially when expressed in the per unit, are very small values. As such, the conductances are rather large numbers. This implies that B_{ii} is rather a negative large in magnitude number. As a reminder, B_{ii} is the sum of the imaginary parts of the line conductances, connecting node i to the neighboring nodes. As such, $\alpha_{q_i}\overline{Q}_i$ is negligible compared to the B_{ii}. Therefore, e_i is a positive quantity.

The (26) implies that $H_{12} = [h_{12_{ij}}]$ and

$$h_{12_{ij}} = \frac{\partial V_i}{\partial \alpha_{q_j}}.$$

It is a known fact in the power systems that injecting more reactive power, increases the line voltages and decreasing the reactive power, reduces the voltages. As such, the change of V and α_q are on the same direction and hence $h_{12_{ij}} > 0$. This implies that H_2 is a square positive matrix.

In most cases $V_i^* < 1$ and as such, f_i in (24) are positive. In cases that V_i^* is greater than unity, yet $1 - V_i^*$ is a small value, in the range of few percents and not larger than 0.05 PU in magnitude. This small value divided by a rather large denominator makes f_i to be small enough not to affect the polarity of EH_{12}. As such, $EH_{12} + F$ is a positive matrix. ■

Theorem 2: It follows from Lemma 1 and Lemma 2 that the system of (31) is asymptotically stable, when β is chosen in such a way that

$$\beta(EH_{12} + F) = c\mathbf{1}\gamma^T + W \quad (34)$$

where

$$0 \leq \|W\| < \sqrt{\|A'\|^2 + \frac{1}{\|P\|}} - \|A'\| \quad (35)$$

where A' is defined by (32) and P is the solution to the following Lyapunov equation:

$$PA' + A'^T P = -I.$$

Proof: Assuming $y_k = \alpha_q(k) - \alpha_q^*$, it follows from (31), (32) and (34) that $y_{k+1} = (A' - W)y_k$. Applying the Lyapunov argument with a Lyapunov function of $V_k = y_k^T P y_k$ yields

$$\begin{aligned}
&V_{k+1} - V_k \\
&= y_k^T[(A' - W)^T P(A' - W) - P]y_k \\
&= y_k^T\{[(A')^T PA' - P] - W^T PA' - (A')^T PW + W^T PW\}y_k \\
&= y_k^T(-I - W^T PA' - (A')^T PW + W^T PW)y_k \\
&\leq (-1 + 2\|P\|\|A'\|\|W\| + \|W\|\|P\|)\|y_k\|^2.
\end{aligned}$$

Since $V_{k+1} - V_k$ is negative definite for all W satisfying (35), system (31) is stable. ■

REFERENCES

[1] H. F. Bilgin and M. Ermis, "Design and implementation of a current-source converter for use in industry applications of d-statcom," *IEEE Trans. Power Electron.*, vol. 25, no. 8, pp. 1943–1957, Aug. 2010.

[2] D. N. Zmood and D. G. Holmes, "Improved voltage regulation for current-source inverters," *IEEE Trans. Ind. Applicat.*, vol. 37, no. 4, pp. 1028–1036, Oct. 2001.

[3] F. Katiraei, M. Iravani, and P. Lehn, "Small-signal dynamics model of a micro-grid including conventional and electronically interfaced distributed resources," *IET Generat., Transmiss., Distribut.*, vol. 1, pp. 369–378, 2007.

[4] F. Katiraei, R. Iravani, N. Hatziargyriou, and A. Dimeas, "Microgrids management," *IEEE Power Energy Mag.*, vol. 6, no. 3, pp. 54–65, May/Jun. 2008.

[5] H. Alatrash, A. Mensah, E. Mark, R. Amarin, and J. Enslin, "Generator emulation controls of photovoltaic inverters," in *Proc. 8th Int. Conf. Power Electron. – ECCE Asia*, Jeju, Korea, May-Jun. 30–3, 2011, pp. 2043–2050.

[6] H. Xin, Z. Qu, J. Seuss, and A. Maknouninejad, "A self-organizing strategy for power flow control of photovoltaic generators in a distribution network," *IEEE Trans. Power Syst.*, vol. 26, no. 3, pp. 1462–1473, Aug. 2011.

[7] P. M. S. Carvalho, P. F. Correia, and L. A. F. M. Ferreira, "Distributed reactive power generation control for voltage rise mitigation in distribution networks," *IEEE Trans. Power Syst.*, vol. 23, no. 3, pp. 766–772, Aug. 2008.

[8] J. Lopes, N. Hatziargyriou, and J. Mutale, "Integrating distributed generation into electric power systems: A review of drivers, challenges and opportunities," *Elect. Power Syst.*, vol. 77, pp. 1189–1203, 2007.

[9] M. E. Baran and I. M. El-Markabi, "A multiagent-based dispatching scheme for distributed generators for voltage support on distribution feeders," *IEEE Trans. Power Syst.*, vol. 22, no. 1, pp. 52–59, Feb. 2007.

[10] T. Nguyen and M. Pai, "A sensitivity-based approach for studying stability impact of distributed generation," *Int. J. Elect. Power Energy Syst.*, vol. 30, pp. 442–446, 2008.

[11] H. Hedayati, S. Nabaviniaki, and A. Akbarimajd, "A method for placement of DG units in distribution networks," *IEEE Trans. Power Del.*, vol. 23, no. 3, pp. 1620–1628, Jul. 2008.

[12] K. D. Brabandere, B. Bolsens, J. V. den Keybus, A. Woyte, J. Driesen, and R. Belmans, "A voltage and frequency droop control method for parallel inverters," *IEEE Trans. Power Electron.*, vol. 22, no. 4, pp. 1107–1115, Jul. 2007.

[13] M. Chandorkar and D. Divan, "Decentralized operation of distributed UPS systems," in *Proc. IEEE PEDES*, 1996, pp. 565–571.

[14] M. Prodanovic and T. Green, "High-quality power generation through distributed control of a power park microgrid," *IEEE Trans. Power Del.*, vol. 53, no. 5, pp. 1471–1482, Oct. 2006.

[15] M. N. Marwali, J.-W. Jung, and A. Keyhani, "Control of distributed generation systems – Part II: Load sharing control," *IEEE Trans. Power Electron.*, vol. 19, no. 6, pp. 1551–1561, Nov. 2004.

[16] F. Katiraei and M. Iravani, "Power management strategies for a microgrid with multiple distributed generation units," *IEEE Trans. Power Syst.*, vol. 21, no. 4, pp. 1821–1831, Nov. 2006.

[17] Y. Abdel-Rady, I. Mohamed, and E. F. El-Saadany, "Adaptive decentralized droop controller to preserve power sharing stability of paralleled inverters in distributed generation microgrids," *IEEE Trans. Power Electron.*, vol. 23, no. 6, pp. 2806–2816, Nov. 2008.

[18] J. C. Vasquez, J. M. Guerrero, A. Luna, P. Rodriguez, and R. Teodorescu, "Adaptive droop control applied to voltage-source inverters operating in grid-connected and islanded modes," *IEEE Trans. Ind. Electron.*, vol. 56, no. 10, pp. 4088–4096, Oct. 2009.

[19] X. Yu, A. Khambadkone, H. Wang, and S. Terence, "Control of parallel-connected power converters for low-voltage microgrid – Part I: A hybrid control architecture," *IEEE Trans. Power Electron.*, vol. 25, no. 12, pp. 2962–2970, Dec. 2010.

[20] J. M. Guerrero, L. G. Vicuna, J. Matas, M. Castilla, and J. Miret, "Output impedance design of parallel-connected ups inverters with wireless load-sharing control," *IEEE Trans. Ind. Electron.*, vol. 52, no. 4, pp. 1126–1135, Aug. 2005.

[21] A. Maknouninejad, Z. Qu, J. Enslin, and N. Kutkut, "Clustering and cooperative control of distributed generators for maintaining microgrid unified voltage profile and complex power control," in *Proc. IEEE PES Transmiss. Distribut. Conf.*, Orlando, FL, USA, May 7–10, 2012, pp. 1–8.

[22] J. Y. Kim, J. H. Jeon, S. K. Kim, C. Cho, J. H. Park, H. M. Kim, and K. Y. Nam, "Cooperative control strategy of energy storage system and microsources for stabilizing the microgrid during islanded operation," *IEEE Trans. Power Electron.*, vol. 25, no. 12, pp. 3037–3048, Dec. 2010.

[23] A. Vaccaro, G. Velotto, and A. F. Zobaa, "A decentralized and cooperative architecture for optimal voltage regulation in smart grids," *IEEE Trans. Ind. Electron.*, vol. 58, no. 10, pp. 4593–4602, Oct. 2011.

[24] A. Nedic and A. Ozdaglar, "Distributed subgradient methods for multi-agent optimization," *IEEE Trans. Autom. Control*, vol. 54, no. 1, pp. 48–61, Jan. 2009.

[25] A. Maknouninejad, W. Lin, H. G. Harno, Z. Qu, and M. A. Simaan, "Cooperative control for self-organizing microgrids and game strategies for optimal dispatch of distributed renewable generations," *Energy Syst.*, vol. 3, pp. 23–60, 2012.

[26] Z. Qu, *Cooperative Control of Dynamical Systems, Applications to Autonomous Vehicles*. London, U.K.: Springer, 2009.

[27] A. Maknouninejad and Z. Qu, "Optimum design and analysis of the cooperative control, applied to the distributed generators control in smart grids," in *Proc. IEEE PES ISGT*, Washington, DC, USA, Feb. 24–27, 2013, pp. 1–6.

[28] Z. Qu and M. Simaan, "A design of distributed game strategies for networked agents," in *Proc. 1st IFAC Workshop Estimat. Control Netw. Syst.*, Venice, Italy, Sep. 24–26, 2009, pp. 270–275.

Ali Maknouninejad (S'08–M'14) received the B.Sc. degree in electrical engineering from the University of Tehran, Tehran, Iran, in 2001 and the M.Sc. degree in electrical engineering and the Ph.D. degree from the University of Central Florida, Orlando, FL, USA, in 2010 and 2013, respectively.

Then, he joined the Power Supply Production (PSP) Co., Tehran, Iran, as a Research Engineer and worked on the design and construction of DC/AC inverter converters up to 30 KVA for use in UPS systems. His research interests include smart grid and distributed generator control and stability analysis.

Zhihua Qu (M'90–SM'93–F'09) received the Ph.D. degree in electrical engineering from the Georgia Institute of Technology, Atlanta, GA, USA, in June 1990.

Since then, he has been with the University of Central Florida (UCF), Orlando, FL, USA. Currently, he is the SAIC Endowed Professor in College of Engineering and Computer Science, Professor and Chair of Electrical and Computer Engineering, and the Director of FEEDER Center (one of DoE-funded national centers on distributed technologies and smart grid). His areas of expertise are nonlinear systems and control, with applications to energy and power systems. In energy systems, his research covers such subjects as low-speed power generation, dynamic stability of distributed power systems, anti-islanding control and protection, distributed generation and load sharing control, distributed VAR compensation, distributed optimization, and cooperative control.